Clinical Epigenetics

RESEARCH

Open Access

HDAC inhibitors modulate Hippo pathway signaling in hormone positive breast cancer

Ting-I Lin[1,2], Yi-Ru Tseng[1,2], Min-Jyun Dong[1,2], Chih-Yi Lin[1,2], Wei-Ting Chung[1,2], Chun-Yu Liu[1,3,4,6], Yi-Fang Tsai[3,4,5], Chi-Cheng Huang[3,4,5], Ling-Ming Tseng[3,4,5], Ta-Chung Chao[1,3,4,6] and Jiun-I Lai[1,2,3,4,6*]

Abstract

Breast cancer has constantly been the leading causes of death in women, and hormone receptor (HR) positive, HER2 negative is the majority subtype. Histone deacetylase (HDAC) inhibitors (HDACi) have shown clinical benefit in HR (+) breast cancer patients. The Hippo pathway is an important cellular pathway involving proliferation, cell contact, and cancer. Hippo pathway proteins YAP/TAZ are often viewed as pro-tumorigenic; however, recent studies support a role of YAP as a tumor suppressor in HR (+) breast cancer. Few studies have investigated the link between HDACi and the Hippo pathway. In our study, we demonstrate that HDACi induces transcriptional downregulation of YAP expression, while conversely activating a TEAD-mediated transcriptional program with upregulation of canonical Hippo pathway genes. We subsequently identified four Hippo canonical genes (CCDC80, GADD45A, F3, and TGFB2) that were upregulated by HDACi and associated with significantly improved survival in a HR (+) breast cancer cohort. We further validated experimentally that HR (+) breast cancer cells treated with HDACi resulted in upregulation of CCDC80 and GADD45A. A pan-cancer analysis of TCGA database demonstrated lower CCDC80 and GADD45A expression in tumor tissue compared to non-tumor samples in BRCA (breast cancer), LAML (acute myeloid leukemia), and UCS (uterine carcinosarcoma). Further analysis of HR (+) breast cancer patients in the METABRIC dataset revealed high CCDC80 and/or GADD45A expression associated with significantly better survival outcomes compared to patients with low expression. Our study provides evidence for a novel mechanism of HDACi clinical activity, as well as a potential role for CCDC80 and GADD45A in HR (+) breast cancer.

Introduction

Breast cancer has constantly been the leading causes of death in women [1, 2], of which the hormone positive (HR(+)) subtype consists of the majority (~70%) [3]. Treatment concept for HR(+) metastatic breast cancer (mBC) currently consists of endocrine therapy (tamoxifen, fulvestrant, and aromatase inhibitors) in addition to targeted therapies (CDK4/6 inhibitors [4–6], PI3K/AKT/mTOR inhibitors [7–9], and histone deacetylase (HDAC) inhibitors (HDACi) [10]), ongoing investigational modalities that including SERCAs (selective estrogen receptor covalent antagonist) [11], CDK7 inhibitors [12], CERANs (complete estrogen receptor antagonists) [13], and others. With the expanding portfolio of molecular-based agents, treatment for HR (+) mBC has improved

Ting-I Lin and Yi-Ru Tseng contributed equally as first authors.

*Correspondence:
Jiun-I Lai
jilai@nycu.edu.tw
[1] Division of Medical Oncology, Department of Oncology, Taipei Veterans General Hospital, Taipei, Taiwan
[2] Institute of Clinical Medicine, National Yang Ming Chiao Tung University, Taipei, Taiwan
[3] School of Medicine, National Yang Ming Chiao Tung University, Taipei, Taiwan
[4] Comprehensive Breast Health Center, Taipei Veterans General Hospital, Taipei, Taiwan
[5] Division of General Surgery, Department of Surgery, Taipei Veterans General Hospital, Taipei, Taiwan
[6] Department of Oncology, Center of Immuno-Oncology, Taipei Veterans General Hospital, Taipei City, Taiwan

significantly in the past decade, although still a far cry from curing this metastatic disease.

Histone deacetylases (HDACs) play a fundamental role in epigenetic modulation of gene expression. Class 1 HDACs inhibit gene transcription by regulating chromatin accessibility and form the core regulatory subunits for gene suppression, including the CoREST, NuRD, Sin3 complexes (containing HDAC1 and HDAC2), and NCoR complex containing HDAC3 [14]. HDACi including vorinostat (SAHA), belinostat (PDX101), romidepsin, and panobinostat (LBH589) have been approved by the FDA for hematological cancers [15–17]. In a phase III clinical trial for HR(+) HER2(−) metastatic breast cancer, the addition of the class I HDACi tucidonistat (chidamide) to aromatase inhibitors demonstrated improved survival [18]. The above clinical results suggest that HDACi may have promising activities in HR (+) breast cancer that warrant further research to realize the maximal therapeutic benefit.

The Hippo pathway is a fundamentally important pathway that governs multiple essential biological functions in cell biology. This includes cell proliferation, organ size, contact inhibition, as well as increasingly reported roles in cancer [19]. Disruption of the Hippo pathway drives carcinogenesis in animal models [20] and in human cancer (comprehensively reviewed in [21]). The canonical Hippo pathway signaling pathway is composed of a phosphorylation cascade including kinases MST1/2, MAP kinases, and LATS1/2 [22], which regulates Yes-associated protein (YAP) and its transcriptional coactivator with PDZ-binding motif (TAZ; also known as WWTR1). YAP and TAZ, well-established major effector proteins of the Hippo pathway [23], can mobilize intranuclearly and bind the transcription factor TEAD, resulting in downstream activation of CTGF, CYR61, ANKRD, and others [24]. YAP/TAZ are generally recognized as oncoproteins and linked to increased oncogenic potential and aggressiveness [25–32], although studies have reported tumor suppressor roles as well [33].

The role of Hippo pathway in epigenetic control of estrogen signaling in HR (+) breast cancer is a topic of intense research. A seminal paper reported LATS1/2 facilitated ESR1 ubiquitination, and LATS1/2 inhibition resulted in YAP/TAZ/ERα (ESR1) activation in HR(+) breast cancer with increased oncogenicity [34]. A conflicting study was recently published showing that LATS1/2 are required to maintain ESR1 expression, and genetic deletion of LATS1/2 stabilizes YAP expression, which, in turn, facilitates VGLL3-TEAD signaling to decreases ESR1 in breast cancer [35]. Since ESR1 was associated with increased tumorigenicity and unfavorable prognosis in HR(+) breast cancer [36, 37], YAP, therefore, seems to play a role as a tumor suppressor in this context [35]. Other recent studies also show LATS1/2 as a tumor promoting role in breast cancer [33, 38]. At this point, it remains inconclusive whether the canonical Hippo pathway signaling of LATS-YAP/TAZ is tumor promoting or suppressing in breast cancer. As studies accumulate rapidly in the Hippo research field, growing evidence suggest a context-dependent different role of the Hippo pathway in cancer [39], requiring additional studies for a concrete conclusion.

The aforementioned study that linked YAP signaling to ESR1 suppression [35] demonstrated that YAP-TEAD activation resulting from LATS1/2 knockout increased VGLL3 expression, which, in turn, recruited NCOR2 repression complex to silence ESR1 expression. The authors also discovered HDACi including entinostat, TSA, and others, increased VGLL3 expression resulting in ESR1 silencing, thus providing a rationale for HDAC inhibitor activity in breast cancer [35], although a direct relationship between HDACi and YAP expression was not described. In another paper from the same research group, the authors described that in small cell lung cancer (SCLC), the benzamide HDACi entinostat (class I HDACi) increased YAP expression, while the pan-HDAC inhibitor TSA did not [40], and TSA could even counter-suppress the activity of entinostat-induced YAP expression. They further proposed a model where in SCLC cells, YAP expression was suppressed by RCOR1/2/3 repression complex, while the SIN3A complex sustained YAP expression that was inhibited by TSA. This intricate regulation surrounding YAP expression suggested that HDACi mechanism of action may be extremely nuanced and context dependent. Adding to the level of complexity, another paper described that HDACi downregulated YAP expression in multiple cancer types [41], in which pan-HDACi were used (LBH589, Dacinostat, TSA, and JNJ-26481585) that showed HDACi decrease of YAP protein expression. The above studies show inconsistent results regarding the relationship between Hippo pathway and HDAC inhibition. Intriguingly, benzamides (of which entinostat belongs to) have demonstrated lower inhibition ability toward Sin3 complexes compared to CoREST and NuRD [14], suggesting that different types of HDACi pharmacore possess distinct preferences of repression complexes which could potentially act as different modes of epigenetic control of Hippo pathway activity.

The above background illustrates the current state of the research regarding Hippo pathway, HDACi and HR (+) breast cancer, with much unanswered questions. We wish to experimentally clarify the role of HDACi and its impact on the Hippo pathway signaling. We also sought to probe how activation of the Hippo pathway and its downstream proteins impact clinical outcome in HR (+)

breast cancer. Interestingly, we discovered that molecularly, HDACi downregulate YAP expression transcriptionally, but conversely heighten TEAD signaling and upregulation of multiple downstream targets. Clinically, the upregulation of several well-known Hippo downstream targets is associated with improved survival in HR (+) breast cancer patients. Our findings provide further insight into the role of Hippo signaling in HR (+) breast cancer as a therapeutically relevant disease pathway and its role in HDACi-mediated clinical efficacy.

Materials and methods

Cell culture and drug treatment

All of the cell lines used in this study were purchased from ATCC Cell Lines (https://www.atcc.org/, with treatment condition as follows: T47D (RPMI-1640, Gibco), MCF-7 (Dulbecco's Modified Eagle Medium (DMEM, Gibco)), MDA-MB-231 (RPMI-1640, Gibco), CAMA-1 (DMEM/F12, Gibco), BT-474 (RPMI-1640, Gibco), and A549 (DMEM/F12, Gibco). All culture medium contained 10% fetal bovine serum (FBS, Gibco) and 1% penicillin–streptomycin (P/S, Gibco). Cells were incubated in 37 °C, 5% CO_2 under standard molecular biology conditions. Romidepsin (Selleck Chemicals, Houston, TX, USA), verteporfin (SML0534, Sigma-Aldrich, Massachusetts, USA), and suberoylanilide hydroxamic acid (SAHA, Cayman Chemicals, Ann Arbor, Michigan) were obtained as solution in dimethyl sulfoxide (DMSO), diluted to 1 mm with DMSO and stored at − 20 °C until further use.

siRNA transfection

siRNA products used in this study were purchased from Thermo Fisher Scientific (Massachusetts, USA). The Lipofectamine™ RNAiMAX was used for siRNA transfection. Cells were seeded with 40–50% confluence in a 6 cm culture dish and mixed with medium without antibiotics. First, each well containing 500 µl of reduced serum Opti-MEM adding 150 pmol siRNA and 6.25 µl RNAiMAX reagent. After 10 min of incubation at room temperature, medium with cells were add into each well and incubated for a duration of 24–72 h at 37 °C using standard cell culture conditions. Cells were then collected for further gene expression analysis.

cDNA preparation and RT-qPCR

T47D or MCF-7 ($5–7\times10^5$ per well) was seeded onto 6 cm dishes. After cell adhesion, cells were treated with the respective drugs (as described in the text and figure legends), washed in PBS and RNA extracted using the TRIzol procedure, resuspended in 35 µL water, and checked for quantity with a Nano-Drop (Thermo Fisher Scientific, RNA with A260/A280 ratios over 1.9 were used.) than stored at − 80 degree. The preparation of cDNA was performed using a HiScript I TM First Strand cDNA Synthesis Kit (Bionovas, Toronto, Canada) following the standardized procedure. For gene expression analysis, RT-qPCR analysis was performed, per standard molecular biology protocols. Sequences of primers are as follows: YAP: Forward: TAGCCCTGCGTAGCC AGTTA, Reverse: TCATGCTTAGTCCACTGTCTGT, CYR61 Forward: AATGGAGCCTCGCATCCTATA, Reverse: TTCTTTCACAAGGCGGCA.

CTGF: Forward: CCCTCGCGGCTTACCGACTGG, Reverse: CACAGGTCTTGGAACAGGCGC,

GAPDH: Forward: GAGTCAACGGATTTGGTCGT, Reverse: GAGGTCAATGAAGGGGTCAT. Data were analyzed using the ΔΔCt method, and statistical significance was determined using a Student's *t*-test.

Western blotting

Cell lysates were subjected to SDS–polyacrylamide gel electrophoresis and subsequently transferred to membranes (Cytiva, Marlborough, MA, USA). Membranes were blocked with a mixture of 5% skimmed milk in PBS for 1 h. Subsequently, they were incubated overnight at 4 °C with primary antibodies specific to YAP (GeneTex, Alton Pkwy Irvine, CA, USA, GTX129151), phosphorylated YAP (Cell Signaling Technology, Danvers, MA, USA, #4911), TAZ (Cell Signaling Technology, Danvers, MA, USA, #4883), GAPDH (Santa Cruz Biotechnology, Dallas, Texas, USA, sc-47724), ESR1 alpha (Cell Signaling Technology, Danvers, MA, USA, #8644), LATS1 (Cell Signaling Technology, Danvers, MA, USA, #3477), and LATS2 (Cell Signaling Technology, Danvers, MA, USA, #5888), with dilutions from 1:500 to 1:3000 in each blocking buffer. After primary antibody incubation with washes by PBST (PBS with 0.1% Tween-20), the membranes were incubated with a secondary antibody conjugated with horseradish peroxidase for 1 h. Protein bands were visualized by using the ECL kit (Millipore, Bedford, MA, USA), and imaging done by GE Amersham Imager 600.

Luciferase assay

Cells were seeded at a density of 4×10^5 cells/well in a 6-well plate and cultured overnight to allow for cell attachment. The luciferase reporter plasmid was then transfected into the target cells using the Lipofectamine™ 3000 system using standard transfection methods, followed by drug treatment. After 48 h of drug treatment, the drug-containing medium was then removed, and cells washed with 1 × PBS, with an appropriate amount of 1 × lysis buffer was added to lyse the cells. An aliquot of 20 µL cell lysate was transferred to a 96-well white plate, and 100 µL luciferase substrate was added, with further

analysis performed on the TECAN SPARK Multimode Microplate Reader. The luciferase expression values were obtained by repeating the reading every 10 s for a total of 10 min. Additionally, 2 µL of cell lysate was used for protein quantification using the BCA Protein Assay Kit, serving as the normalization for each well.

The plasmid used for the luciferase assay is the 8xGTIIC-luciferase, a gift from Stefano Piccolo (Addgene plasmid # 34,615; http://n2t.net/addgene:34615; RRID:Addgene_34615) [42]. Briefly, this plasmid utilizes a synthetic TEAD luciferase reporter that is activated when TEAD binds to the TEAD-binding site, indicating functional TEAD-based transcription [42].

Immunofluorescence

Cells were cultured on Millicell® EZ SLIDES (Millipore, Bedford, MA, USA), fixed in 4% paraformaldehyde for 10 min at room temperature, and extracted with 0.2% Triton X-100 solution for 10 min. After blocking with phosphate-buffered saline with Tween-20 (PBST) containing 1% bovine serum albumin for 30 min, the cells were incubated with YAP antibody overnight at 4℃. Cells were washed for three times with PBST and then incubated with fluorescein isothiocyanate conjugated secondary antibody for 1 h. After that, cells were counterstained with Fluoroshield™ with DAPI (Sigma-Aldrich, Burlington, MA) to visualize the nucleus. The coverslips were mounted onto glass slides with an anti-fade solution and subjected to the examination under an Olympus FV10i confocal microscope.

RNA-sequencing

T47D or MCF-7 ($5–7\times10^5$ per well) was seeded onto 6 cm dish and treated with romidepsin or vehicle for 5 days, washed in PBS, and RNA was extracted (Total RNA Isolation Kit, NovelGene). RNA was checked for quantity with a Nano-Drop (Thermo Fisher Scientific, RNA with A260/A280 ratios over 1.9 were used.) than stored at − 80 °C. Libraries were prepared using a TruSeq Stranded mRNA sample preparation kit (Illumina, San Diego, CA) from 500 ng of purified total RNA according to the manufacturer's protocol in a reduced reaction volume. The finished cDNA libraries were assessed for quality using a Bioanalyzer and quantified with a Quant-iT dsDNA Assay kit (Thermo Fisher Scientific, Waltham, MA). The uniquely indexed libraries were multiplexed based on this quantitation, and the pooled sample was quantified by qPCR using the Kapa Biosystems (Wilmington, MA) library quantification kit by the Molecular Biology Core Genomics Facility at the Dana-Farber Cancer Institute and sequenced on a single Illumina NextSeq500 run with single-end 75 bp reads. Reads were processed to counts using the bcbio-Nextgen toolkit version 1.0.3a (https://github.com/chapmanb/bcbio-nextgen) as follows: (1) Reads were trimmed and clipped for quality control in cutadapt v1.12; (2) read quality was checked for each sample using FastQC 0.11.5; (3) high-quality reads were then aligned into BAM files through STAR 2.5.3a using the human assembly GRCh37; and (4) BAM files were imported into DEXSeq-COUNT 1.14.2, and raw counts TPM and RPKM were calculated. R package edgeR (McCarthy et al., 2012; Robinson et al., 2010) 3.18.1 (R version 3.2.1) was used for differential analysis and generate log fold change, p-value, and FDR.

The RNA-seq results were deposited into the Gene Expression Omnibus (GEO) database under the accession number GSE263971.

Survival analysis, pathway analysis, and data processing

DAVID analysis was performed on the DAVID website (https://david.ncifcrf.gov/tools.jsp). Survival analysis was performed on cBioPortal website (https://www.cbioportal.org/) [43] using the METABRIC dataset [44]. To select HR (+) HER2(-) only patient samples, from the METABRIC dataset, "Breast Invasive Ductal Carcinoma" was firstly chosen, followed by selection of "mRNA expression z-scores relative to all samples," "ER status positive," and "HER2 status negative." After filtering, clinical and mRNA data were downloaded from the remaining samples, with removal of samples with unavailable overall survival data, yielding a total of 1030 samples. The C-G high expression cohort was selected with patients' samples with either CCDC80 or GADD45A consisting of a positive z-score (> 0), with the remaining samples defined as the C-G low expression cohort. Sample IDs from each the C-G high and C-G low cohort were retrieved and input into cBioPortal as 2 non-overlapping groups for further analysis. The complete list of each cohort is uploaded as supplementary files. A similar approach was used to filter HER2 cohort (selection of HER2 status positive) and TNBC cohort (selection of ER status negative, HER2 status negative).

The transcriptome datasets used in this study include: GSE69845, GSE72688, GSE133120, GSE70120, GSE74478, and GSE263971, each downloaded from GEO and processed by R. The cell type for each dataset is as follows:

GSE69845: microarray data of MCF-7 cells treated with Vorinostat/SAHA 100 nM for 6 h. Three biological repeats for each vehicle and treatment were available and used for analysis.

GSE263971: (data from our current study) RNA-seq data of MCF-7 and T47D cells treated with romidepsin 50 nM for 24 h, two biological repeats for each vehicle and treatment were available and used for analysis.

GSE72688: microarray data of MDA-MB-231 cells treated with vorinostat 5 uM for 24 h. Three biological repeats pairs used.

GSE133120: microarray data of MDA-MB-231 cells treated with romidepsin 46 nM for 6 h. Three biological repeats pairs used.

GSE70120: microarray data of UM-UC-3 or VM-CUB-1 cells, treated with 3 nM romidepsin, 0.5 uM givinostat, and 2.5 uM SAHA, each for 24 h, three biological repeats.

GSE74478: microarray data of VM-CUB1 treated with siRNA against HDAC1 and HDAC2, normalized to VM-CUB1 with nontargeting siRNA, three biological repeats.

For the microarray datasets, the dataset was analyzed by the web-based tool GEO2R [45] to produce the differential expression list.

Heat maps, gene ontology (GO) analysis, dot plot, and ridge plot were generated by the R packages "ClusterProfiler," "enrichplot," "pHeatmap," and "GSEAplot."

GEPIA analysis

The cross-TCGA dataset analysis was performed using the GEPIA2 webserver database [46]. A total of 31 TCGA datasets were included in GEPIA2 and were used for our analysis. The full list of datasets include: ACC (Adrenocortical carcinoma), BLCA (Bladder urothelial carcinoma), BRCA (Breast invasive carcinoma), CESC (Cervical squamous cell carcinoma and endocervical adenocarcinoma), CHOL (Cholangiocarcinoma), COAD (Colon adenocarcinoma), DLBC (Lymphoid neoplasm diffuse large B-cell lymphoma), ESCA (Esophageal carcinoma), GBM (Glioblastoma multiforme), HNSC (Head and neck squamous cell carcinoma), KICH (Kidney chromophobe), KIRC (Kidney renal clear cell carcinoma), KIRP (Kidney renal papillary cell carcinoma), LAML (Acute myeloid leukemia), LGG (Brain lower grade glioma), LIHC (Liver hepatocellular carcinoma), LUAD (Lung adenocarcinoma), LUSC (Lung squamous cell carcinoma), OV (Ovarian serous cystadenocarcinoma), PAAD (Pancreatic adenocarcinoma), PCPG (Pheochromocytoma and paraganglioma), PRAD (Prostate adenocarcinoma), READ (Rectum adenocarcinoma), SARC (Sarcoma), SKCM (Skin cutaneous melanoma), STAD (Stomach adenocarcinoma), TGCT (Testicular germ cell tumors), THCA (Thyroid carcinoma), THYM (Thymoma), UCEC (Uterine corpus endometrial carcinoma), and UCS (Uterine carcinosarcoma).

Results

Transcriptional profiling of HDACi reveals suppression of cell cycle pathways and upregulation of canonical Hippo pathway targets

To specifically investigate the global transcriptomic changes by HDACi in HR (+) breast cancer cells, we performed RNA-sequencing in T47D and MCF-7, both HR (+) HER2(-) breast cancer cell lines, with the class I HDAC inhibitor romidepsin [47]. To mitigate the confounding effect on individual cell line characteristics that would impact the results, we overlapped genes that were both differentially expressed in MCF-7 and T47D. In both cell lines, nearly ~ 6000 genes were differentially expressed (twofold difference, $p < 0.05$, adjusted $p < 0.05$), with an overlap of 3512 genes (Fig. 1A). We filtered out genes that changed in opposing directions between the two lines (i.e., only genes that were concurrently up- or down-regulated in both cell lines were selected), resulting in 3366 genes chosen for further analysis. Gene ontology (GO) analysis revealed pathways relating to cell cycle (including chromosome segregation, mitosis, DNA replication, nuclear division, and others) as leading pathways, indicating that romidepsin strongly perturbs the cell cycle in HR (+) breast cancer (Fig. 1B). Consistently, KEGG pathways associated with romidepsin treatment revealed that the cell cycle was significantly and substantially suppressed as shown by dot plot and ridge plot (Fig. 1C, D), and GSEA analysis showed cell cycle pathway strongly suppressed with NES of -3.59 (Fig. 1E). DAVID analysis also showed cell cycle as the top over-represented pathways (Fig. 1F), where interestingly, the Hippo pathway was also among the leading enriched pathways. The association of HDACi and cell cycle pathways have been well studied [48]; however, the discovery of the Hippo pathway in the leading pathways was interesting and relatively unknown.

We sought to investigate the expression profile of a previously reported Hippo pathway gene signature set [49] in our RNA-seq data. We observed that in both cell lines, treatment of romidepsin resulted in upregulation in majority of the signature Hippo pathway downstream genes in both cell lines, including the canonical CYR61/CCN1, CTGF/CCN2, NUAK2, GADD45A, and others (Fig. 1G, H). Notably, the Hippo pathway component LATS2 was upregulated in MCF-7 cells (Fig. 1H), but downregulated in T47D cells (Fig. 1G), suggesting that cell line intrinsic differences resulted in inconsistent transcription responses to HDACi.

In conclusion, RNA-seq of HR (+) breast cancer cell lines treated with romidepsin revealed a strong suppression of the cell cycle-related pathways and enriched Hippo pathway expression and signaling, as well as confirming that conventional TEAD expression targets such as CYR61 and CTGF are upregulated.

HDAC inhibitors activate TEAD transcription while transcriptionally suppress YAP expression

We then performed experiments to validate our findings from the RNA-seq data. HR (+) breast cancer cell lines treated with romidepsin revealed upregulation in

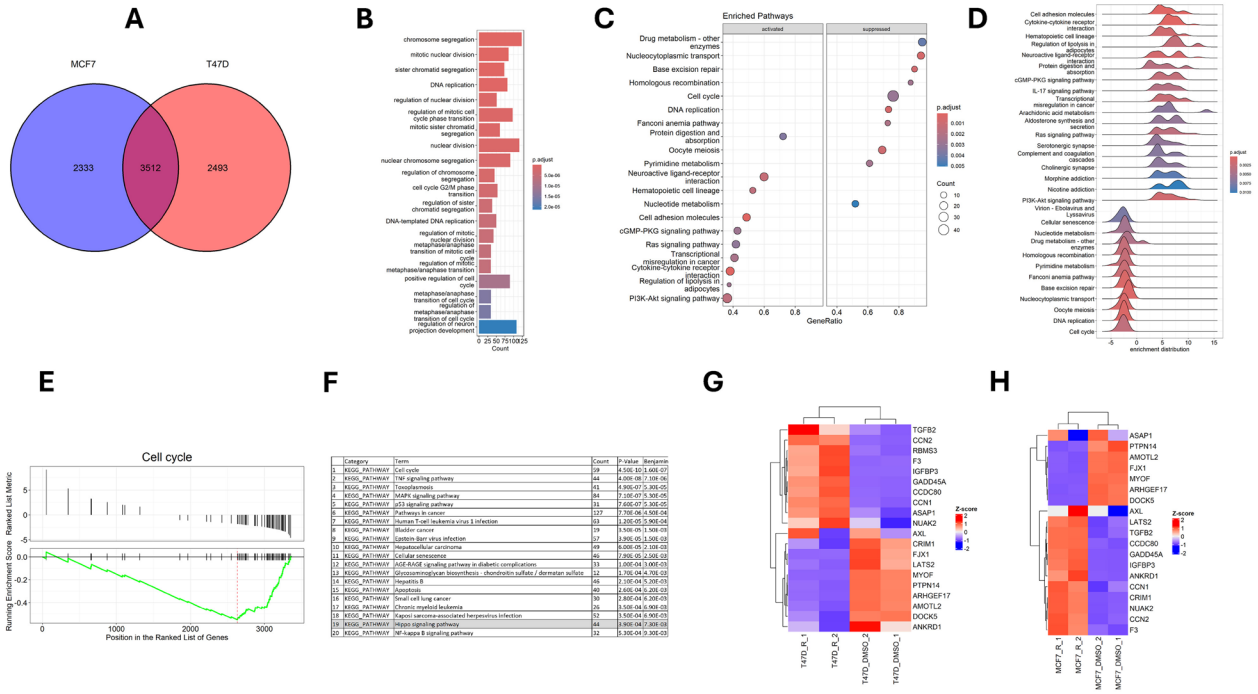

Fig. 1 RNA-seq of HR(+) breast cancer cells treated with romidepsin reveals pathway enrichment including cell cycle and Hippo pathways. **A** Venn diagram of differentially expressed genes (DEG) from RNA-seq data performed on MCF-7 or T47D cells, treated with either romidepsin 50 nM or DMSO for 24 h. **B**–**D** Gene ontology (GO) analysis (**B**), dot plot (**C**), and ridge plot (**D**) of DEGs from the RNA-seq data. **E** GSEA analysis for cell cycle pathway from the RNA-seq data. **F** Leading enriched pathways from DAVID analysis of the RNA-seq data. **G**, **H** Heat map of mRNA expression from the RNA-seq dataset of Hippo pathway signature genes [49] in T47D (**G**) and MCF-7 (**H**)

CYR61, CTGF (Fig. 2A), consistent with our prior findings. We then asked whether HDAC inhibitors activated TEAD-based transcription. We used the 8xGTIIC-TEAD luciferase reporter, a well-established reporter assay for investigating TEAD-mediated transcription [42], in breast cancer cell lines treated with HDACi. We observed that TEAD luciferase reporter activity upregulated significantly after HDACi treatment (Fig. 2B), in both MCF-7 and T47D cell lines, as well as A549, a lung cancer cell line, suggesting that this phenomenon is not limited to breast cancer. To validate this finding across multiple cell lines, we queried the GEO database for transcriptional profiling datasets where various cancer cell lines were treated with HDACi, including: MCF-7 (HR(+) breast cancer) treated with SAHA (Vorinostat) (GSE69845), romidepsin (GSE263971, our current study), T47D (HR(+) breast cancer) treated with romidepsin, (GSE263971, our current study) MDA-MB-231 (TNBC) treated with SAHA (GSE72688), romidepsin (GSE133120), VM-CUB1 (bladder cancer), and UM-UC-3 cells (bladder cancer) treated with the HDACi romidepsin, givinostat, SAHA, and siRNAs against HDAC1/2 (GSE70120, GSE74478). mRNA expressions for CTGF and CYR61 were largely upregulated compared to controls, with some differences between cell lines (Fig. 2C). Notably, the upregulation occurred more substantially in HDACi-treated cell lines, especially with romidepsin and givinostat (a class I/II HDAC inhibitor [50]); however, siRNA against HDAC1/2 showed modest increase in CTGF and CYR61 expression. Our findings indicate that HDAC inhibition activates TEAD-based transcription in the Hippo pathway and upregulates Hippo pathway canonical targets, including CYR61 and CTGF.

Our above data demonstrate that HDACi activates TEAD-based transcription in the Hippo pathway. Interestingly, the previous research has shown that class I HDACi downregulate YAP protein expression in cancer cells [41], but whether this is mediated at the transcriptional level is unclear from the study. When we treated multiple cell lines with romidepsin, including the HR (+) HER2(−) breast cancer cell lines MCF-7, T47D, CAMA-1, as well as the HER2(+) cell line BT-474, triple negative breast cancer cell line (TNBC) MDA-MB-231, and the lung cancer cell line A549, we observed a significant downregulation of YAP expression (Fig. 2D). This suppression in YAP expression was time dependent (Fig. 2E). The canonical Hippo pathway is based on

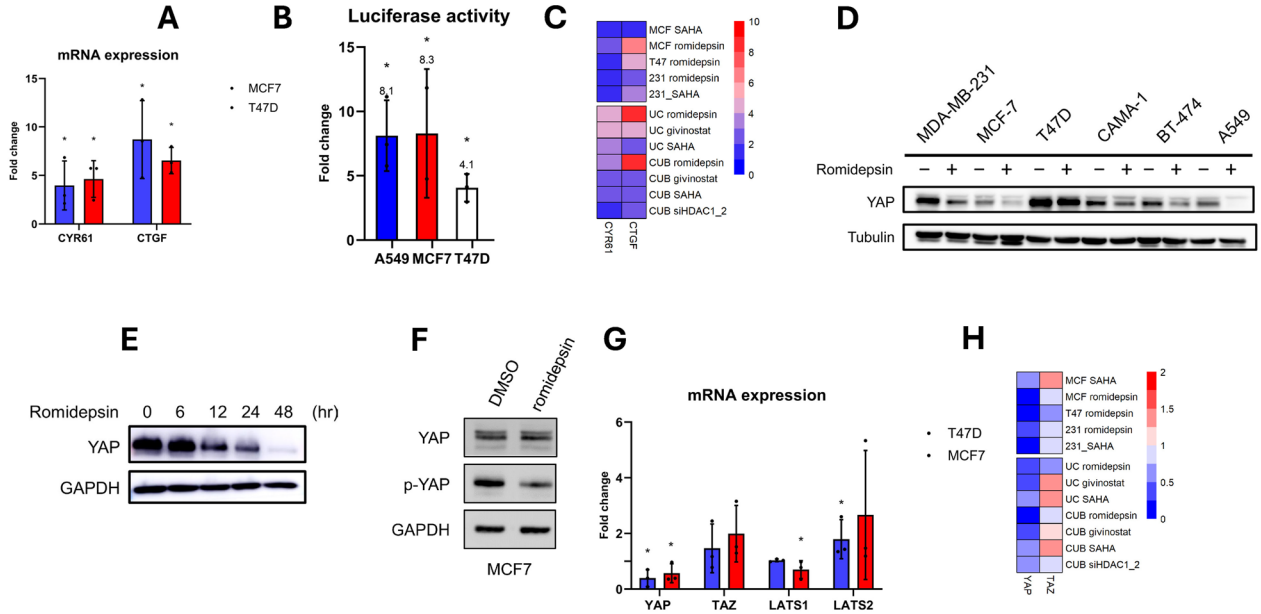

Fig. 2 HDACi upregulates Hippo pathway targets CYR61, CTGF, and TEAD luciferase reporter activity, while downregulating YAP expression. **A** MCF-7 and T47D cells were treated with romidepsin 50 nM for 24 h. qRT-PCR was performed for quantification of CYR61 and CTGF mRNA. Fold change (Y-axis) represents fold change of romidepsin-treated cells compared to DMSO-treated cells. Each dot represents a biological replicate (i.e., this experiment repeated 3 times). Blue: MCF-7. Red: T47D. *sign denotes $p < 0.05$. **B** A549, MCF-7, and T47D treated with romidepsin 50 nM and measured for luciferase activity by the 8xGTIIC-TEAD luciferase reporter. Activity fold changes normalized to DMSO-treated cells. Each dot represents a biological replicate (3 repeats for each cell line). (**C**) Heat map of mRNA expression of CTGF and CYR61 from the transcriptome datasets (see methods for full list). Abbreviations for cell lines: MCF: MCF-7 HR (+) breast cancer cell line. T47: T47D HR (+) breast cancer cell line. 231: MDA-MB-231 (TNBC). CUB: VM-CUB1 urothelial cancer cell line. UC: UM-UC-3 urothelial cancer cell line. SAHA: Vorinostat. siHDAC1_2: treated with combination of siRNAs against HDAC1 and HDAC2. Color palette denotes fold change compared to individual controls. **D** Multiple cell lines treated with romidepsin 30 nM for 24 h and blotted for YAP expression. Plus sign denotes treatment with romidepsin, minus sign denotes treatment with DMSO. (Romidepsin 30 nM was chosen for immunoblotting studies as this concentration demonstrated consistent changes across cell lines tested) **E** T47D cells treated with romidepsin 30 nM at various time points and blotted for YAP expression. **F** MCF-7 treated with romidepsin 30 nM for 24 h and blotted for YAP, phosphorylated YAP (p-YAP). **G** MCF-7 and T47D cells treated by romidepsin 30 nM for 24 h. qRT-PCR was performed for quantification of YAP1, TAZ, LATS1, and LATS2 mRNA. Fold change (Y-axis) represents fold change of romidepsin-treated cells compared to DMSO-treated cells. Each dot represents a biological replicate (Total 3 biological repeats). Blue: MCF-7. Red: T47D. *sign denotes $p < 0.05$. **H** Heat map of mRNA expression of TAZ and YAP from the transcriptome datasets (see methods for full list). Cell line denotation described in legend for Fig. 2C. Color palette denotes fold change compared to individual controls

phosphorylation of YAP, which directs it to cytoplasmic destruction instead of intranuclear translocation. Interestingly, romidepsin or SAHA treatment decreased phosphorylated YAP in MCF-7 and A549 cell lines (Fig. 2F, supplementary Fig. 1A). To test whether this suppression occurred at the transcriptional level, we treated MCF-7 and T47D with romidepsin for 24 h and observed significant downregulation of YAP1 mRNA, while there were no substantial decrease (and even mild increase), in TAZ, LATS1, or LATS2 mRNA levels (Fig. 2G).

Since both YAP mRNA and phosphorylated YAP are downregulated, our data suggest that HDACi decrease YAP by a transcriptomic silencing mechanism instead of protein degradation mediated by the canonical Hippo pathway. We analyzed again the aforementioned transcriptomic datasets and observed a consistent downregulation of YAP mRNA after treatment with HDAC inhibition (Fig. 2H), while TAZ expression was not decreased, and even mildly increased. Compared to the substantial decrease of YAP expression, the expression of LATS1/2 showed very minor changes (Fig. supp 1B). Taken together with the above data, we conclude that HDAC inhibition results in transcription suppression of YAP expression but conversely activates TEAD-mediated transcription of Hippo pathway targets. One possible explanation was despite global YAP downregulation, intranuclear YAP was increased, leading to upregulation of YAP-TEAD transcription. However, we did not observe increased intranuclear YAP expression by immunofluorescence (Fig. supp 1C).

A recent study described that HDACi entinostat, SAHA, and CORIN resulted in ESR1 downregulation in MCF-7 cells ([35], supplementary Fig. 2A). We confirmed this observation by treating T47D cells with romidepsin,

SAHA, and entinostat. Our data revealed that these HDACi suppressed ESR1 expression in a dose-dependent fashion (supplementary Fig. 2A). There was a consistent downregulation of YAP/TAZ protein expression with all three HDACi, as well as ESR1 (supplementary Fig. 2B). In summary, our data indicate that HDACi result in YAP expression downregulation at the transcriptional level and also induce ESR1 protein downregulation.

Identification of Hippo pathway downstream genes associated with improved survival outcomes in HR (+) breast cancer

Our previous results identified that romidepsin treatment resulted in upregulation of several Hippo pathway signature genes. Specifically, a total of nine genes (*TGFB2, CYR61/CCN1, CTGF/CCN2, TGFB2, CCDC80, GADD45A, IGFBP3, NUAK2, and F3*) were significantly upregulated in both T47D and MCF-7 treated with romidepsin. We asked whether the expression was correlated with survival in HR (+) breast cancer in large sample size transcriptomic datasets. From the METABRIC cohort [44], we selected cases that were HR(+) HER2(−) and contained available mRNA expression data, with a total of 1030 cases selected. When categorized into high versus low gene expression for each gene in this cohort, we discovered that expression of four genes (*CCDC80, GADD45A, F3, and TGFB2*) was significantly correlated with overall survival. Strikingly, all four genes demonstrated a significant association of higher gene expression level with better overall survival (p-value < 0.05) (Fig. 3A, supp Fig. 3A). In the cases of *GADD45* ($p < 0.0001$, overall survival in high versus low expression: 199 versus 142 months) and *CCDC80* ($p = 0.0022$, overall survival in high versus low expression: 178.2 versus 148.8 months), the differences in survival were more substantial.

We hypothesized that gene expression levels of GADD45 and/or CCDC80 would be significant prognostic factors for HR (+) breast cancer, and we sought to further explore clinical characteristics of patients with higher expression of either of these genes. From the above 1030 cases, we categorized the patients into high expression (of either GADD45 and/or CCDC80) and low expression groups. High and low expression groups each contained 587 and 443 patients, respectively. Clinical characteristics of the two groups were examined through the cBioPortal database. As expected, high expression patients (High C-G) had significantly longer survival compared to low expression patients (Low C-G) (185 months versus 132.1 months, hazard ratio 0.71, $p = 0.00002$) (Fig. 3B). Relevant clinical characteristics revealed no significant difference between PR status, tumor stage, positive lymph nodes, type of breast surgery, neoplasm histologic grade, and tumor size (supplementary file 1); interestingly, when applying the 3-gene classifier [51], the low C-G group had significantly more patients with high proliferation ER + HER2- profile, indicating a more proliferative nature of cancer (Fig. 3C). Recurrence free survival was also significantly longer in the C-G high group ($p = 0.01$) (Fig. 3D).

Since our current analysis was restricted to HR (+) breast cancer, we investigated whether expression levels of either CCDC80/GADD45A or CTGF, CYR61 were associated with outcome difference in other subtypes of breast cancer. By further analysis of METABRIC, there was no significant association between gene expression of CCDC80, GADD45A, CTGF, CYR61, and survival in HER2(+) or TNBC patients (supplementary Fig. 3B, C).

To validate our findings mechanistically, we examined the expression of CCDC80 and GADD45A in the transcriptomic datasets from Fig. 2C. We discovered a consistent upregulation in both GADD45A and CCDC80 gene expression after various HDACi treatments (Fig. 3E). To further validate this finding experimentally, we examined the levels of CCDC80 and GADD45A subsequent to romidepsin treatment. Consistent with the above findings, we observed that romidepsin-induced upregulation of GADD45A (Fig. 3F), and more substantially, CCDC80 (Fig. 3G), in both MCF-7 and T47D cells. Verteporfin is a small molecule discovered through a drug screening program and proven to inhibit YAP-TEAD protein interaction, thus suppressing YAP-mediated TEAD activity [52]. Verteporfin is now widely used as tool for investigation regarding biological mechanisms of the Hippo-TEAD signaling pathway [53, 54]. Since our current data indicate that HDACi upregulate TEAD-based transcription, shown by the luciferase reporter assay and RNA-seq data, we hypothesized that treatment with verteporfin could shed light on whether CCDC80 and GADD45A was mechanistically regulated by TEAD transcription. We treated T47D and MCF-7 with verteporfin and observed, consistent with prior knowledge, downregulation of CYR61 expression, indicating that Hippo-TEAD transcription was suppressed (Fig. 3H). Interestingly, CCDC80 showed strong downregulation in both cell lines, and GADD45A also was downregulated in MCF-7, although not in T47D, suggesting cell line differences.

We then sought to investigate whether siRNA against HDAC1/2 could replicate the findings of HDACi as described above. We treated MCF-7 cells with two pairs of siRNAs (each pair containing a siRNA against HDAC1 and a siRNA against HDAC2). Interestingly, we observed a decrease in YAP expression after treatment with both siHDAC1/2 pairs; however, we did not observe the substantial upregulation of CCDC80 and GADD45A expression (supplementary Fig. 4A). We then asked whether knockdown

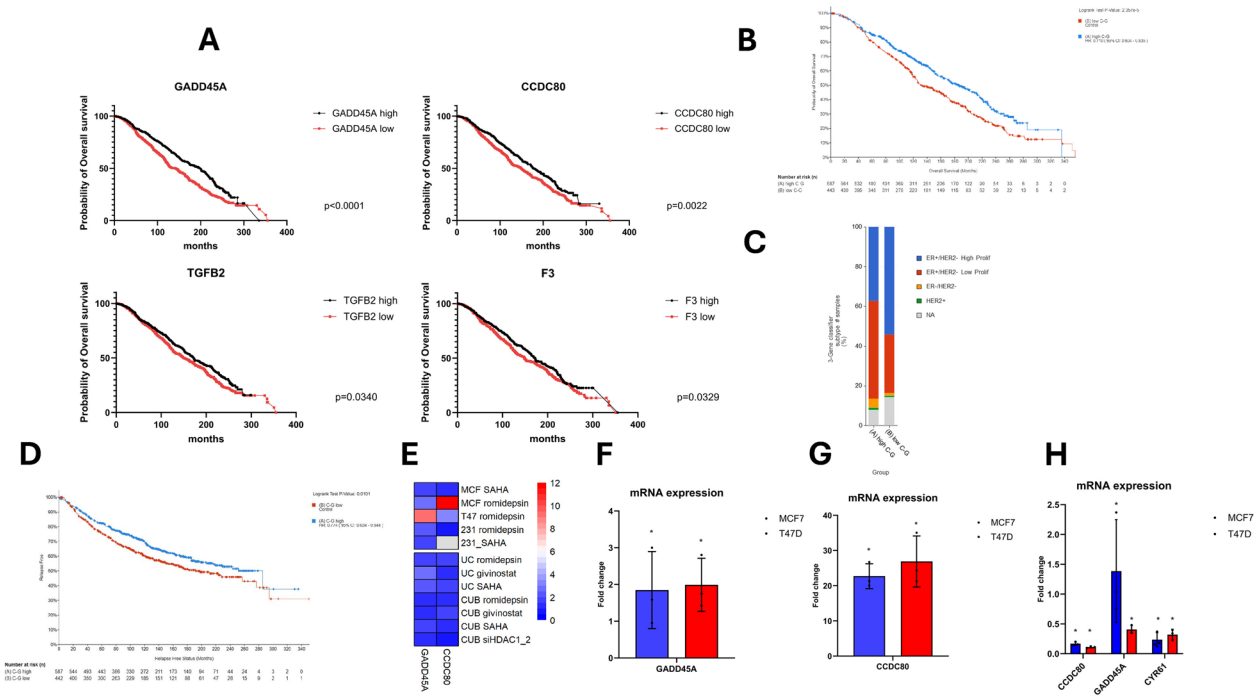

Fig. 3 Hippo pathway downstream genes CCDC80 and GADD45A are associated with survival in HR (+) breast cancer. **A** Overall survival analysis for genes GADD45A, CCDC80, F3, and TGFB2 from the TCGA METABRIC dataset, filtered for HR (+) HER2(-) breast cancer cases. mRNA expression levels were downloaded for each patient sample and categorized into 1:1 ratio of high expression versus low expression, followed by comparison of overall survival. **B** Overall survival (OS) curves between patients with high expression of CCDC80 or GADD45A (High C-G) versus low expression (Low C-G). **C** Three-gene classifier for intrinsic subtype distribution between high C-G patients versus low C-G patients. **D** Recurrence free survival (RFS) curves between patients with high expression of CCDC80 or GADD45A (High C-G) versus low expression (Low C-G). **E** Heat map of mRNA expression of CCDC80 and GADD45A from the transcriptome datasets (see methods for full list). Cell line denotation described in legend for Fig. 2C. Color palette denotes fold change compared to individual controls. **F**, **G** MCF-7 and T47D treated with romidepsin 50 nM for 24 h. qRT-PCR was performed for quantification of GADD45A and CCDC80 mRNA. Fold change (Y-axis) represents fold change of romidepsin-treated cells compared to DMSO-treated cells. **H** MCF-7 and T47D treated with verteporfin 4 μM for 24 h. In Fig. 3F–H, each dot represents a biological replicate (i.e., repeated 3 times), blue bars and red bars are MCF-7 and T47D, respectively. *sign denotes $p < 0.05$

of YAP alone would also affect CCDC80 and GADD45A expression. Although significant knockdown was achieved by 2 siRNAs targeting YAP, there was only modest down-regulation of CCDC80 expression, and mild upregulation of GADD45A (supplementary Fig. 4B).

To summarize, romidepsin substantially increases GADD45A and CCDC80 expression (Fig. 3F), and verteporfin, a Hippo pathway inhibitor, produces opposite results (Fig. 3H). siRNA against HDAC1/2 did not reproduce the same findings as romidepsin, compatible with the previous microarray studies (Fig. 3E). This finding indicates a discrepancy between chemical inhibition and genetic silencing for HDAC1/2, which could be explained by other factors (such as compensatory mechanisms in response to siHDAC1/2).

Pan-cancer transcriptomic analysis reveals upregulation of CCDC80 and GADD45A in tumor tissue in breast cancer patient samples

To further investigate the pan-cancer distribution of CCDC80 and GADD45A, we queried the GEPIA2 web browser [46] for a cross-cancer type analysis of TCGA datasets. Thirty-one cancer types were analyzed (see methods for full list of cancer types). In tumor tissues, 10 datasets (BLCA, BRCA, CESC, COAD, LAML, OV, PRAD, READ, UCEC, and UCS) exhibited significantly reduced expression levels of CCDC80 (Fig. 4A, supp 4C), while four datasets (BRCA, LAML, SKCM, and UCS) demonstrated significantly decreased expression levels of GADD45A compared to their expression in normal tissues (Fig. 4B, supp 4D). Overall, three datasets had

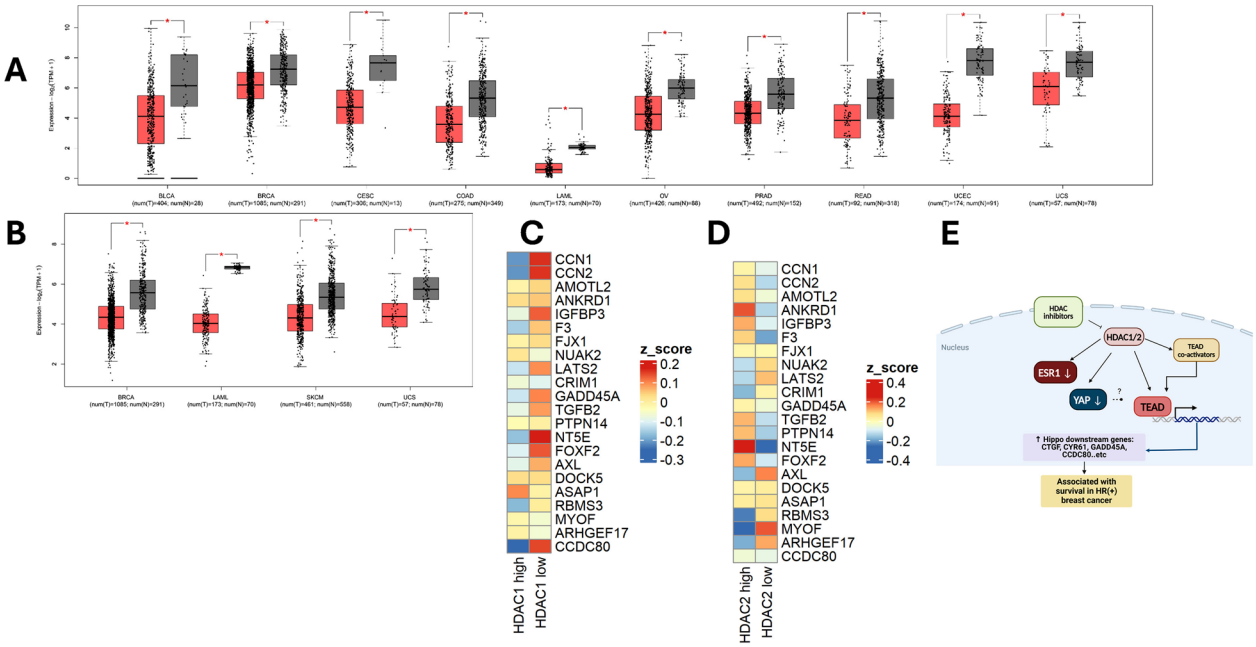

Fig. 4 Pan-cancer transcriptomic analysis reveals upregulation of CCDC80 and GADD45A in tumor tissue in breast cancer patient samples. **A**, **B** Comparison of tumor and normal samples for CCDC80 expression (**A**) or GADD45A expression (**B**), from 31 TCGA datasets, analyzed by GEPIA2 web browser database. Datasets showing decreased CCDC80 expression in tumor versus normal are shown here. **C** Comparison of Hippo pathway genes between HDAC1 high versus HDAC1 low patient samples analyzed from the METABRIC database. **D** Comparison of Hippo pathway genes between HDAC2 high versus HDAC2 low patient samples analyzed from the METABRIC database. **E** Proposed mechanism for this study. In our current working model, HDAC inhibitors result in downregulation of YAP and ESR1 expression transcriptionally, while activating TEAD-based transcriptional activation of Hippo pathway downstream genes including CCDC80 and GADD45A. Higher expression of CCDC080 and GADD45A is associated with improved outcomes in HR(+) HER2(−) breast cancer

consistent trend for CCDC80 and GADD45A (downregulated expression in tumor samples): BRCA (Breast invasive carcinoma), LAML (Acute myeloid leukemia), and UCS (Uterine carcinosarcoma). Conversely, six datasets (CHOL, DLBC, GBM, LGG, LIHC, and PAAD) and two datasets (GBM and PAAD) had significantly higher expression in tumor samples for CCDC80 and GADD45A, respectively (supplementary Fig. 4C, D).

We further analyzed whether HDAC1/2 expression in METABRIC was associated with differences in activation of Hippo pathway targets. We divided the patients by high/low expression of HDAC1 or HDAC2 mRNA levels from the METABRIC dataset. In patients with low HDAC1 expression, there was marked upregulation in the Hippo pathway genes, including CYR61/CCN1, CTGF/CCN2, CCDC80, GADD45A, NT5E, IGFBP3, and several others (Fig. 4C), compared to patient samples with high HDAC1 expression. The trend was less clear between HDAC2 high and low expression patient samples (Fig. 4D). Our data indicate a possible association between HDAC1 expression levels and activation of Hippo pathway genes.

Taken together the above, our findings show consistent results that HDAC inhibitors results in upregulation of the Hippo pathway targets GADD45A and CCDC80 (in both our RNA-seq data and the GSE70120 and GSE74478 datasets), and high CCDC80 or GADD45A expression is associated with more favorable survival outcomes in HR(+) HER2(-) breast cancer (from the METABRIC dataset [44]) with less aggressive cancer biology (lower proliferation). We further validated that GADD45A and especially CCDC80 are upregulated by HDACi, and downregulated by the Hippo-TEAD inhibitor verteporfin, indicating the role of Hippo-TEAD signaling in this axis. We summarized our findings from this study in a mechanistic illustration (Fig. 4E).

Discussion

Even with the advent of CDK4/6 inhibitors, metastatic hormone positive breast cancer still remains incurable, with patients ultimately succumbing to the disease. There is still a huge unmet need for therapeutic agents such as HDACi that are efficacious in treatment for HR (+) breast cancer. The treatment of HR (+) breast cancer is unique that besides cytotoxic chemotherapy and targeted therapy (such as PI3K/AKT/mTOR inhibitors), therapeutics that disrupt estrogen signaling or ESR1 expression provide clinical benefit in HR (+) breast cancer patients.

The previous studies have demonstrated HDACi-mediated ESR1 downregulation [55, 56], likely through upregulation of transcriptional repressors for ESR1 [57]. This hypothesis is supported by the recent study that delineates HDACi upregulation of VGLL3 which recruits silencing complexes that suppress ESR1 expression [35]. In general, HDACi may exert cytotoxicity in HR(+) breast cancer by multiple mechanisms including ESR1 downregulation [55, 56], induction of intrinsic CDK inhibitors such as p21 [58], induction of p53 resulting in cancer cell apoptosis [59], and others. Although clinical trials using HDACi have had both successes and failures in phase III trials (including the ACE trial [18] and the E2112 trial [60]), HDACi still remains a viable option for treatment in HR(+) breast cancer, and further understanding of the underlying mechanism will further unlock the potential for therapeutics avenues.

Accumulating recent evidence now supports the notion that Hippo pathway signaling, especially YAP/TAZ-TEAD signaling, may not be uniformly oncogenic, rather it is more likely that the Hippo pathway may be context dependent in terms of oncogenicity. In our study, we discovered that despite HDACi suppression of YAP expression, as evidenced by our cell line data, RNA-seq data, and publicly available GEO datasets, TEAD signaling is activated, and the majority of Hippo signature genes [49] are upregulated, including the conventional Hippo-TEAD targets CYR61 and CTGF [61]. CYR61 and CTGF were proposed as mediators for paclitaxel resistance [61] and are generally considered as oncogenic [62, 63]. However, from our RNA-seq data, we observed that other Hippo pathway signature genes are modulated as well, suggesting that HDACi induce an intricate transcriptional perturbation effect on Hippo pathway transcriptome. Interestingly, we discover that GADD45A and CCDC80 as highly prognostic of improved survival in HR (+) HER2(-) breast cancer patients. GADD45A and CCDC80 are well-established targets of Hippo-TEAD signaling [49, 64, 65]. GADD45A is associated with luminal type breast cancer, highly positive in HR + cancers and low in normal or HER2/TNBC [66], plays a role in cell cycle regulation [67], and was previously reported as directly induced by HDACi [68]. Most studies have shown that GADD45A is pro-apoptosis and plays a role in tumor killing [69, 70]. Few studies have reported the role of CCDC80 in cancer. A recent study reported tumor-suppressive role of CCDC80 in colon cancer cell lines [65]. Interestingly, this study reported an oncogenic role of LATS1/2 [65], in which the authors speculate is context dependent. Taken together the findings from our study and others [71, 72], we speculate that the context-dependent role of the Hippo pathway in cancer, i.e., whether oncogenic or tumor-suppressive, is dependent upon the amplitude of expression induced for Hippo targets that possess anti-tumor properties, such as CCDC80 and GADD45A. As CCDC80 is relatively under-investigated in cancer, further studies will be beneficial to further characterize its role as a prognostic and/or therapeutic potential. Our findings provide, at least partially, a possible explanation for HDACi efficacy in HR (+) breast cancer and propose a previously undiscovered HDAC-TEAD-CCDC80/GADD45A axis that could serve as potential biomarkers or therapeutic development in HR (+) breast cancer. More interestingly, the pan-cancer analysis across 31 cancer types revealed that only three cancer types (breast cancer, acute myeloid leukemia, and uterine carcinosarcoma) share the trend of having lower tumor expression of CCDC80 and GADD45A, suggesting future investigation on whether these two genes have a prognostic role or whether the Hippo signaling through these two genes serve as a tumor-suppressive role in these three cancer types.

In our study, we showed that HDACi downregulated YAP (Fig. 3C–G), but upregulated expression of Hippo canonical genes (Figs. 2A, C and 3E–G). Although detailed molecular mechanisms remain unknown, data in our study may shed some light on these two seemingly counterintuitive conclusions. In the canonical Hippo pathway, YAP/TAZ both are capable of binding and activating the transcription factor TEAD, suggesting a functional redundancy. Some studies have shown that YAP/TAZ reciprocally increase with the counterpart is genetically silenced [73]. In our data, we observed a modest increase (around 1.5-fold compared to control) of TAZ mRNA expression when treated with HDACi, while YAP was significantly suppressed (Fig. 3D, E). However, when we looked at the protein level, TAZ expression was consistently suppressed after HDACi treatment (Fig. 3C, Supplementary 1A), arguing against compensatory activation of TEAD by TAZ. One possible scenario is HDACi induce strong upregulation of TEAD-binding partners, including VGLL proteins, AP-1 transcription factor family (FOS, JUN, and others). Indeed, in our RNA-seq data, we observed consistent increase in both cell lines upregulation of FOS, JUN, and JUND (data not illustrated. Complete RNA-seq data deposited to GEO). We speculate that HDACi, by downregulation of YAP/TAZ, and upregulating potential TEAD coactivators, create an environment that favors nuclear accumulation of TEAD coactivators and thus turning on TEAD transcription. A similar model has been shown recently, where upregulation of VGLL3, a TEAD co-factor, results in silencing of the ESR1 gene [35]. In this scenario, VGLL3 replaces TEAD to mediate transcription, but facilitates transcriptional suppression instead of activation. Interestingly, in our

RNA-seq data, VGLL3 was upregulated as well, providing an explanation for ESR1 downregulation in our data (supplementary Fig. 2A, B).

In our data, HDACi including romidepsin, SAHA, and entinostat all downregulated YAP expression. Since romidepsin is a specific HDAC1/2 inhibitor, we were curious whether simultaneous knockdown of HDAC1/2 could recapitulate the transcriptional changes. However, from our experiments (supplementary Fig. 4A, B) as well as from the GEO transcriptomic datasets, siHDAC1/2 showed the least amount of YAP downregulation (Fig. 2H), least amount of CTGF/CYR61 (2C) and CCDC80/GADD45A upregulation (3E), in comparison with HDACi. Mechanistically, there remains a fundamental gap between siRNA against HDAC1/2 and HDACi in terms of biological consequences. HDAC1 has a long half-life, and prior studies have shown that downstream consequences by HDAC1/2 gene deletion (stable double knockout) are most marked after 96 h of gene inactivation [74]. Theoretically, siHDAC1/2 at less than 96 h would produce insufficient levels of knockdown of HDAC1/2, which among themselves have high levels of homology and functional redundancy [75, 76], thus blunting the possible downstream effect. HDACi, on contrary, start to inhibit the HDAC enzymatic activity as soon as HDAC-small-molecule engagement is achieved [77]. Other potential factors, including off target effects that may be present in both small molecules and siRNA, may also contribute to the inconsistency of the biological readout. As our study utilizes multiple cell lines and HDACi and largely achieving consistent observations, we believe that the inconsistency by the siHDAC1/2, both in the GEO datasets and in our experiments, may be partially explained by the above, and does not contradict the main findings of our study.

In summary, our study provides novel insights into the role of the Hippo pathway and HDACi in HR (+) breast cancer. We discover that while HDACi downregulates YAP, TEAD signaling is heightened that upregulates several downstream genes of the Hippo pathway linked to improved survival. Our findings provide possible mechanisms for HDACi role in HR(+) breast cancer, and hint toward potential novel targeting agents, such as LATS inhibitors [35], Hippo pathway modulating agents, or further exploitation of CCDC80 and GADD45A, to improve outcomes and survival for this group of patients.

Supplementary Information

The online version contains supplementary material available at https://doi.org/10.1186/s13148-025-01834-y.

Supplementary file

Acknowledgements
The authors thank the funding agencies (NSTC, Taiwan Clinical Oncology Research Foundation, the Melissa Lee Cancer Foundation, Taipei Veterans General Hospital) for support.

Author contributions
TIL, YRT, and JIL designed the experiments. TIL, YRT, MJD, CYL, WTC, and JIL performed the experiments and prepared the figures. CYL, YFT, CCH, LMT, TCC, and JIL discussed, reviewed, and revised clinical aspects of the manuscript. TIL, YRT, and JIL drafted and wrote the manuscript. All authors reviewed the manuscript.

Funding
This study was partially funded by the grants to JIL: NSTC 112–2314-B-A49-054 (National Science and Technology Council, Taiwan), the Taiwan Clinical Oncology Research Foundation, the Melissa Lee Cancer Foundation, and 112DHA0100294 (Taipei Veterans General Hospital internal grant).

Data availability
The RNA-seq results were deposited into the Gene Expression Omnibus (GEO) database under the accession number GSE263971.

Declarations

Ethics approval and consent to participate
Ethics approval and consent to participate as below.

Consent for publication
No individual patient data or sample were used in this study, with the exception of the public database from METABRIC [44] and GEPIA2 database (described in methods). Data analyses were in compliance with cBioPortal (https://www.cbioportal.org/) data analysis guidelines.

Competing interests
The authors declare no competing interests.

Received: 1 May 2024 Accepted: 4 February 2025
Published online: 26 February 2025

References

1. Siegel RL, Miller KD, Jemal A. Cancer statistics, 2020. CA Cancer J Clin. 2020;70(1):7–30.
2. Duggan C, Trapani D, Ilbawi AM, Fidarova E, Laversanne M, Curigliano G, et al. National health system characteristics, breast cancer stage at diagnosis, and breast cancer mortality: a population-based analysis. Lancet Oncol. 2021;22(11):1632–42.
3. Perou CM, Sorlie T, Eisen MB, van de Rijn M, Jeffrey SS, Rees CA, et al. Molecular portraits of human breast tumours. Nature. 2000;406(6797):747–52.
4. Goetz MP, Toi M, Campone M, Sohn J, Paluch-Shimon S, Huober J, et al. MONARCH 3: abemaciclib as initial therapy for advanced breast cancer. J Clin Oncol Off J Am Soc Clin Oncol. 2017;35(32):3638–46.
5. Hortobagyi GN, Stemmer SM, Burris HA, Yap YS, Sonke GS, Paluch-Shimon S, et al. Ribociclib as first-line therapy for HR-positive, advanced breast cancer. N Engl J Med. 2016;375(18):1738–48.
6. Finn RS, Martin M, Rugo HS, Jones S, Im SA, Gelmon K, et al. Palbociclib and letrozole in advanced breast cancer. N Engl J Med. 2016;375(20):1925–36.
7. Jones RH, Casbard A, Carucci M, Cox C, Butler R, Alchami F, et al. Fulvestrant plus capivasertib versus placebo after relapse or progression on an aromatase inhibitor in metastatic, oestrogen receptor-positive breast cancer (FAKTION): a multicentre, randomised, controlled, phase 2 trial. Lancet Oncol. 2020;21(3):345–57.
8. Andre F, Ciruelos E, Rubovszky G, Campone M, Loibl S, Rugo HS, et al. Alpelisib for PIK3CA-mutated, hormone receptor-positive advanced breast cancer. N Engl J Med. 2019;380(20):1929–40.

9. Baselga J, Campone M, Piccart M, Burris HA 3rd, Rugo HS, Sahmoud T, et al. Everolimus in postmenopausal hormone-receptor-positive advanced breast cancer. N Engl J Med. 2012;366(6):520–9.
10. Wang J, Xu B. Targeted therapeutic options and future perspectives for HER2-positive breast cancer. Signal Transduct Target Ther. 2019;4(1):34.
11. Hamilton EP, Wang JS, Pluard TJ, Johnston SRD, Morikawa A, Dees EC, Jones RH, Haley BB, Armstrong AC, Cohen AL, Munster PN, Wright GLS, Kayali F, Korpal M, Xiao JA, Long J, Destenaves B, Gao L, Gualberto A, Juric D. Phase I/II study of H3B-6545, a novel selective estrogen receptor covalent antagonist (SERCA), in estrogen receptor positive (ER+), human epidermal growth factor receptor 2 negative (HER2-) advanced breast cancer. ASCO Annual Meeting 2021.
12. Howell SJ, MGK, Lord S, Kenny L, Bahl A, Clack G, Ainscow E, Arkenau H, Mans JL, Palmieri C, Richards P, Jeselsohn R, Mitri Z, Gradishar WJ, Sardesai S, O'Shaughnessy J, Lehnert M, Ali S, McIntosh S, Coombes RC. 265P - Study of samuraciclib (CT7001), a first-in-class, oral, selective inhibitor of CDK7, in combination with fulvestrant in patients with advanced hormone receptor positive HER2 negative breast cancer (HR+BC). European Society for Medical Oncology 2021.
13. Lin NU, Borges VF, Patel MR, Okera M, Meisel J, Wesolowski R, et al. 382MO Updated results from the phase I/II study of OP-1250, an oral complete estrogen receptor (ER) antagonist (CERAN) and selective ER degrader (SERD) in patients (pts) with advanced or metastatic ER-positive, HER2-negative breast cancer. 2023.
14. Bantscheff M, Hopf C, Savitski MM, Dittmann A, Grandi P, Michon AM, et al. Chemoproteomics profiling of HDAC inhibitors reveals selective targeting of HDAC complexes. Nat Biotechnol. 2011;29(3):255–65.
15. Iyer SP, Foss FF. Romidepsin for the treatment of peripheral T-cell lymphoma. Oncologist. 2015;20(9):1084–91.
16. Richardson PG, Laubach JP, Lonial S, Moreau P, Yoon SS, Hungria VT, et al. Panobinostat: a novel pan-deacetylase inhibitor for the treatment of relapsed or relapsed and refractory multiple myeloma. Expert Rev Anticancer Ther. 2015;15(7):737–48.
17. Autin P, Blanquart C, Fradin D. Epigenetic drugs for cancer and microrna: a focus on histone deacetylase inhibitors. Cancers (Basel). 2019;11(10):1530.
18. Jiang Z, Li W, Hu X, Zhang Q, Sun T, Cui S, et al. Tucidinostat plus exemestane for postmenopausal patients with advanced, hormone receptor-positive breast cancer (ACE): a randomised, double-blind, placebo-controlled, phase 3 trial. Lancet Oncol. 2019;20(6):806–15.
19. Harvey KF, Zhang X, Thomas DM. The Hippo pathway and human cancer. Nat Rev Cancer. 2013;13(4):246–57.
20. Halder G, Johnson RL. Hippo signaling: growth control and beyond. Development. 2011;138(1):9–22.
21. Zanconato F, Cordenonsi M, Piccolo S. YAP/TAZ at the roots of cancer. Cancer Cell. 2016;29(6):783–803.
22. Meng Z, Moroishi T, Guan KL. Mechanisms of Hippo pathway regulation. Genes Dev. 2016;30(1):1–17.
23. Moroishi T, Hayashi T, Pan WW, Fujita Y, Holt MV, Qin J, et al. The Hippo pathway kinases LATS1/2 suppress cancer immunity. Cell. 2016;167(6):1525.
24. Harvey K, Tapon N. The Salvador-Warts-Hippo pathway - an emerging tumour-suppressor network. Nat Rev Cancer. 2007;7(3):182–91.
25. Eisinger-Mathason TS, Mucaj V, Biju KM, Nakazawa MS, Gohil M, Cash TP, et al. Deregulation of the Hippo pathway in soft-tissue sarcoma promotes FOXM1 expression and tumorigenesis. In: Proceedings of the National academy of sciences of the United States of America. 2015;112(26):E3402-11
26. Lu T, Li Z, Yang Y, Ji W, Yu Y, Niu X, et al. The Hippo/YAP1 pathway interacts with FGFR1 signaling to maintain stemness in lung cancer. Cancer Lett. 2018;423:36–46.
27. Li Z, Wang Y, Zhu Y, Yuan C, Wang D, Zhang W, et al. The Hippo transducer TAZ promotes epithelial to mesenchymal transition and cancer stem cell maintenance in oral cancer. Mol Oncol. 2015;9(6):1091–105.
28. Song S, Honjo S, Jin J, Chang SS, Scott AW, Chen Q, et al. The Hippo coactivator YAP1 Mediates EGFR overexpression and confers chemoresistance in esophageal cancer. Clin Cancer Res Off J Am Assoc Cancer Res. 2015;21(11):2580–90.
29. Cottini F, Hideshima T, Xu C, Sattler M, Dori M, Agnelli L, et al. Rescue of Hippo coactivator YAP1 triggers DNA damage-induced apoptosis in hematological cancers. Nat Med. 2014;20(6):599–606.
30. Chan LH, Wang W, Yeung W, Deng Y, Yuan P, Mak KK. Hedgehog signaling induces osteosarcoma development through Yap1 and H19 overexpression. Oncogene. 2014;33(40):4857–66.
31. Janse van Rensburg HJ, Azad T, Ling M, Hao Y, Snetsinger B, Khanal P, et al. The Hippo pathway component TAZ promotes immune evasion in human cancer through PD-L1. Cancer Res. 2018;78(6):1457.
32. Elaimy AL, Guru S, Chang C, Ou J, Amante JJ, Zhu LJ, et al. VEGF-neuropilin-2 signaling promotes stem-like traits in breast cancer cells by TAZ-mediated repression of the Rac GAP beta2-chimaerin. Sci Signal. 2018. https://doi.org/10.1126/scisignal.aao6897.
33. Fan H, Wang X, Li W, Shen M, Wei Y, Zheng H, et al. ASB13 inhibits breast cancer metastasis through promoting SNAI2 degradation and relieving its transcriptional repression of YAP. Genes Dev. 2020;34(19–20):1359–72.
34. Britschgi A, Duss S, Kim S, Couto JP, Brinkhaus H, Koren S, et al. The Hippo kinases LATS1 and 2 control human breast cell fate via crosstalk with ERalpha. Nature. 2017;541(7638):541–5.
35. Ma S, Tang T, Probst G, Konradi A, Jin C, Li F, et al. Transcriptional repression of estrogen receptor alpha by YAP reveals the Hippo pathway as therapeutic target for ER(+) breast cancer. Nat Commun. 2022;13(1):1061.
36. Furth PA, Wang W, Kang K, Rooney BL, Keegan G, Muralidaran V, et al. Overexpression of estrogen receptor alpha in mammary glands of aging mice is associated with a proliferative risk signature and generation of estrogen receptor alpha-positive mammary adenocarcinomas. Am J Pathol. 2023;193(1):103–20.
37. Denkert C, Loibl S, Kronenwett R, Budczies J, von Torne C, Nekljudova V, et al. RNA-based determination of ESR1 and HER2 expression and response to neoadjuvant chemotherapy. Ann Oncol. 2013;24(3):632–9.
38. Li Q, Sun Y, Jarugumilli GK, Liu S, Dang K, Cotton JL, et al. Lats1/2 sustain intestinal stem cells and Wnt activation through TEAD-dependent and independent transcription. Cell Stem Cell. 2020;26(5):675–92.
39. Li FL, Guan KL. The two sides of Hippo pathway in cancer. Semin Cancer Biol. 2021. https://doi.org/10.1016/j.semcancer.2021.07.006.
40. Wu Z, Su J, Li FL, Chen T, Mayner J, Engler A, et al. YAP silencing by RB1 mutation is essential for small-cell lung cancer metastasis. Nat Commun. 2023;14(1):5916.
41. Han H, Yang B, Nakaoka HJ, Yang J, Zhao Y, Le Nguyen K, et al. Hippo signaling dysfunction induces cancer cell addiction to YAP. Oncogene. 2018;37(50):6414–24.
42. Dupont S, Morsut L, Aragona M, Enzo E, Giulitti S, Cordenonsi M, et al. Role of YAP/TAZ in mechanotransduction. Nature. 2011;474(7350):179–83.
43. Sherman BT, Hao M, Qiu J, Jiao X, Baseler MW, Lane HC, et al. DAVID: a web server for functional enrichment analysis and functional annotation of gene lists (2021 update). Nucleic Acids Res. 2022;50(W1):W216–21.
44. Curtis C, Shah SP, Chin SF, Turashvili G, Rueda OM, Dunning MJ, et al. The genomic and transcriptomic architecture of 2,000 breast tumours reveals novel subgroups. Nature. 2012;486(7403):346–52.
45. Barrett T, Wilhite SE, Ledoux P, Evangelista C, Kim IF, Tomashevsky M, et al. NCBI GEO: archive for functional genomics data sets–update. Nucleic Acids Res. 2013;41:D991.
46. Tang Z, Kang B, Li C, Chen T, Zhang Z. GEPIA2: an enhanced web server for large-scale expression profiling and interactive analysis. Nucleic Acids Res. 2019;47(W1):W556–60.
47. Wagner JM, Hackanson B, Lubbert M, Jung M. Histone deacetylase (HDAC) inhibitors in recent clinical trials for cancer therapy. Clin Epigenetics. 2010;1(3–4):117–36.
48. Zhang HS, Gavin M, Dahiya A, Postigo AA, Ma D, Luo RX, et al. Exit from G1 and S phase of the cell cycle is regulated by repressor complexes containing HDAC-Rb-hSWI/SNF and Rb-hSWI/SNF. Cell. 2000;101(1):79–89.
49. Wang Y, Xu X, Maglic D, Dill MT, Mojumdar K, Ng PK, et al. Comprehensive molecular characterization of the Hippo signaling pathway in cancer. Cell Rep. 2018;25(5):1304.
50. Sonthalia M, Roy BS, Chandrawanshi D, Ganesh GV, Jayasuriya R, Mohandas S, et al. Histone deacetylase inhibitors as antidiabetic agents: advances and opportunities. Eur J Pharmacol. 2022;935:175328.
51. Haibe-Kains B, Desmedt C, Loi S, Culhane AC, Bontempi G, Quackenbush J, et al. A three-gene model to robustly identify breast cancer molecular subtypes. J Natl Cancer Inst. 2012;104(4):311–25.
52. Liu-Chittenden Y, Huang B, Shim JS, Chen Q, Lee SJ, Anders RA, et al. Genetic and pharmacological disruption of the TEAD-YAP complex suppresses the oncogenic activity of YAP. Genes Dev. 2012;26(12):1300–5.

53. Calses PC, Crawford JJ, Lill JR, Dey A. Hippo pathway in cancer: aberrant regulation and therapeutic opportunities. Trends Cancer. 2019;5(5):297–307.
54. Zhang H, Ramakrishnan SK, Triner D, Centofanti B, Maitra D, Gyorffy B, et al. Tumor-selective proteotoxicity of verteporfin inhibits colon cancer progression independently of YAP1. Sci Signal. 2015;8(397):ra98.
55. Bicaku E, Marchion DC, Schmitt ML, Munster PN. Selective inhibition of histone deacetylase 2 silences progesterone receptor-mediated signaling. Can Res. 2008;68(5):1513–9.
56. deFazio A, Chiew YE, Donoghue C, Lee CS, Sutherland RL. Effect of sodium butyrate on estrogen receptor and epidermal growth factor receptor gene expression in human breast cancer cell lines. J Biol Chem. 1992;267(25):18008–12.
57. Raha P, Thomas S, Thurn KT, Park J, Munster PN. Combined histone deacetylase inhibition and tamoxifen induces apoptosis in tamoxifen-resistant breast cancer models, by reversing Bcl-2 overexpression. Breast Cancer Res. 2015;17(1):26.
58. Ju R, Muller MT. Histone deacetylase inhibitors activate p21(WAF1) expression via ATM. Can Res. 2003;63(11):2891–7.
59. Wang H, Zhou W, Zheng Z, Zhang P, Tu B, He Q, et al. The HDAC inhibitor depsipeptide transactivates the p53/p21 pathway by inducing DNA damage. DNA Repair. 2012;11(2):146–56.
60. Yeruva SLH, Zhao F, Miller KD, Tevaarwerk AJ, Wagner LI, Gray RJ, et al. E2112: randomized phase iii trial of endocrine therapy plus entinostat/placebo in patients with hormone receptor-positive advanced breast cancer. NPJ Breast Cancer. 2018;4:1.
61. Lai D, Ho KC, Hao Y, Yang X. Taxol resistance in breast cancer cells is mediated by the hippo pathway component TAZ and its downstream transcriptional targets Cyr61 and CTGF. Can Res. 2011;71(7):2728–38.
62. Yin S, Jin W, Qiu Y, Fu L, Wang T, Yu H. Solamargine induces hepatocellular carcinoma cell apoptosis and autophagy via inhibiting LIF/miR-192-5p/CYR61/Akt signaling pathways and eliciting immunostimulatory tumor microenvironment. J Hematol Oncol. 2022;15(1):32.
63. Kim H, Son S, Ko Y, Shin I. CTGF regulates cell proliferation, migration, and glucose metabolism through activation of FAK signaling in triple-negative breast cancer. Oncogene. 2021;40(15):2667–81.
64. Passaro F, De Martino I, Zambelli F, Di Benedetto G, Barbato M, D'Erchia AM, et al. YAP contributes to DNA methylation remodeling upon mouse embryonic stem cell differentiation. J Biol Chem. 2021;296:100138.
65. Pan WW, Moroishi T, Koo JH, Guan KL. Cell type-dependent function of LATS1/2 in cancer cell growth. Oncogene. 2019;38(14):2595–610.
66. Tront JS, Willis A, Huang Y, Hoffman B, Liebermann DA. Gadd45a levels in human breast cancer are hormone receptor dependent. J Transl Med. 2013;11:131.
67. Hollander MC, Fornace AJ Jr. Genomic instability, centrosome amplification, cell cycle checkpoints and Gadd45a. Oncogene. 2002;21(40):6228–33.
68. Hirose T, Sowa Y, Takahashi S, Saito S, Yasuda C, Shindo N, et al. p53-independent induction of Gadd45 by histone deacetylase inhibitor: coordinate regulation by transcription factors Oct-1 and NF-Y. Oncogene. 2003;22(49):7762–73.
69. Wang X, Hao Y, Chen J, Ding P, Lv X, Zhou D, et al. Nuclear complement C3b promotes paclitaxel resistance by assembling the SIN3A/HDAC1/2 complex in non-small cell lung cancer. Cell Death Dis. 2023;14(6):351.
70. Hu Y, Jin R, Gao M, Xu H, Zou S, Li X, et al. Transcriptional repression of IKKbeta by p53 in arsenite-induced GADD45alpha accumulation and apoptosis. Oncogene. 2019;38(5):731–46.
71. Traboulsi T, El Ezzy M, Dumeaux V, Audemard E, Mader S. Role of SUMOylation in differential ERalpha transcriptional repression by tamoxifen and fulvestrant in breast cancer cells. Oncogene. 2019;38(7):1019–37.
72. Nait Achour T, Sentis S, Teyssier C, Philippat A, Lucas A, Corbo L, et al. Transcriptional repression of estrogen receptor alpha signaling by SENP2 in breast cancer cells. Mol Endocrinol. 2014;28(2):183–96.
73. Patterson MR, Cogan JA, Cassidy R, Theobald DA, Wang M, Scarth JA, et al. The Hippo pathway transcription factors YAP and TAZ play HPV-type dependent roles in cervical cancer. Nat Commun. 2024;15(1):5809.
74. Jamaladdin S, Kelly RD, O'Regan L, Dovey OM, Hodson GE, Millard CJ, et al. Histone deacetylase (HDAC) 1 and 2 are essential for accurate cell division and the pluripotency of embryonic stem cells. In: Proceedings of the national academy of sciences of the United States of America. 2014;111(27):9840-9845
75. Montgomery RL, Davis CA, Potthoff MJ, Haberland M, Fielitz J, Qi X, et al. Histone deacetylases 1 and 2 redundantly regulate cardiac morphogenesis, growth, and contractility. Genes Dev. 2007;21(14):1790–802.
76. Yamaguchi T, Cubizolles F, Zhang Y, Reichert N, Kohler H, Seiser C, et al. Histone deacetylases 1 and 2 act in concert to promote the G1-to-S progression. Genes Dev. 2010;24(5):455–69.
77. Xu C, Soragni E, Chou CJ, Herman D, Plasterer HL, Rusche JR, et al. Chemical probes identify a role for histone deacetylase 3 in Friedreich's ataxia gene silencing. Chem Biol. 2009;16(9):980–9.

Publisher's Note